A first-principles study of the β''-phase in Al-Mg-Si alloys

2002 J. Phys.: Condens. Matter 14 4011

(http://iopscience.iop.org/0953-8984/14/15/315)

INSTITUTE OF PHYSICS PUBLISHING JOURNAL OF PHYSICS: CONDENSED MATTER

J. Phys.: Condens. Matter **14** (2002) 4011–4024 PII: S0953-8984(02)32958-8

A first-principles study of the β''-phase in Al–Mg–Si alloys

P M Derlet[1,2,5], S J Andersen[3], C D Marioara[1,4] and A Frøseth[1]

[1] Department of Physics, Norwegian University of Science and Technology (NTNU), N-7034 Trondheim, Norway
[2] Paul Scherrer Institute, CH-5232 Villigen PSI, Switzerland
[3] SINTEF Materials Technology, Applied Physics, N-7050 Trondheim, Norway
[4] National Centre for HREM, Laboratory of Materials Science, Delft University of Technology, Rotterdamseweg 137, 2628 Al Delft, The Netherlands

E-mail: peter.derlet@psi.ch

Received 23 January 2002, in final form 13 March 2002
Published 4 April 2002
Online at stacks.iop.org/JPhysCM/14/4011

Abstract

Al–Mg–Si alloys gain an increase in strength due to small precipitates of Mg and Si formed from the solid-solution phase, where maximum hardness arises from a combination of a large number of fully coherent Guinier–Preston (GP) 1 zones and semi-coherent GP 2 zones (the β''-Mg_5Si_6 phase), both existing as needle-like structures. In the present work we investigate the nature of bonding within the equivalent bulk structure of the β''-phase, using the density functional theory technique. In particular we investigate the presence of covalent bonding between Si using the calculated charge-density/transfer distributions of the structure. In addition we find small residual Hellmann–Feynman forces on the atoms, and accordingly relax the structure and find a more symmetric structure in terms of geometry and charge density. We find also that the converged structure is stable against atomic position perturbations that break the inversion and mirror plane symmetries of the $C2/m$ β''-phase. Finally we investigate a face-centred-cubic array of only Mg and Si atoms—a candidate model for the GP 1 phase, from which the β''-structure may be recovered by a simple transformation and subsequent atomic relaxation.

1. Introduction

The normally accepted precipitation sequence in the Al–Mg–Si alloy system [1–4] is: SSSS $\rightarrow$ atomic clusters with Mg, Si $\rightarrow$ GP 1 zones $\rightarrow$ GP 2 zones (β'') $\rightarrow$ $\beta' \rightarrow \beta$, where SSSS refers to the initial supersaturated solid solution and GP a Guinier–Preston (GP) zone. This sequence is generally thought to apply in the temperature range 150–250 °C. Although it is not

[5] Author to whom any correspondence should be addressed.

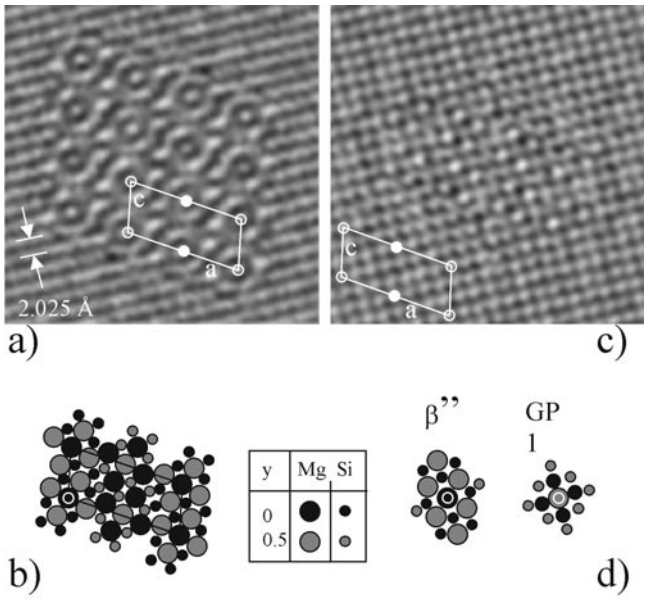

Figure 1. (*a*) An exit wave image of the β''-phase with an overlay of the unit cell of β''. (*b*) A sketch of the atomic structure model of β''. Big/small circles represent Mg/Si atoms. The two atomic layers are grey or black. (*c*) An exit wave image of a GP 1 zone with Mg and Si atoms arranged near Al FCC positions. The GP 1 unit-cell overlay is shown in the Al matrix. (*d*) The atomic motif around central Mg atoms in the GP 1 and β''-phases. In the GP 1 the four 'bright atoms' are Al (intermediate-size circles) or Mg atoms arranged in a square centred above a Mg atom. A displacement $b/2$ of this atom in the β''-structure will let all atoms become arranged on a distorted FCC array, giving a model for the GP 1 structure.

confirmed, the β^n-phases are considered to contain no Al. As a general rule, during the heat treatment, the next β^n-phase to form is richer in Mg than the previous one. This means that unless there exist additional phases in the sequence, some of the Si must have been initially removed from solution at a much higher rate than Mg. The sequence also depends naturally on the initial composition. At equilibrium when the final phase β (Mg_2Si) is reached and no excess Mg remains in solution, then if the overall Mg/Si ratio is <2, crystals of Si will coexist with β.

Zandbergen, Andersen and co-workers [5, 6] have identified the crystallography of the so-called β''-phase in the Al–Mg–Si alloy system (see figure 1(*a*)), by using solely electron microscopy techniques. This Mg_5Si_6 phase is believed to be responsible, in part, for the increased strength and hardness properties of the commercial series-6000 Al alloys. Such GP 2 zones exist as needles, providing optimal material strength via the pinning of dislocations. Recently the crystallography of the GP 1 zone (or the pre-β''-phase) has also been published [7] (see figure 1(*c*)). On the basis of the analysis of the interatomic distances, the published GP 1 structure was found, in this case, to contain Al.

The excess number of vacancies and the supersaturation of Mg and Si atoms in the Al matrix are due to a rapid cooling from an elevated temperature (400–500 °C), for example, after an extrusion. The nature of these early atomic clusters is still unresolved. Atom-probe field-ion-microscopy experiments [8, 9] indicate that the most common clusters contain only Si or a combination of Mg and Si, and to a lesser extent pure Mg. Subsequent storage at room temperature (RT), but prior to the heat treatment (ageing), or a slow heating to the precipitation

temperature (common procedures in the industry), greatly influence the precipitation and growth of β''. When there is a supersaturation, nucleation of Mg–Si clustering in the Al matrix will take place even for temperatures below RT. Only recently have quantitative data on the precipitates at RT begun to appear [10]. Thus, in spite of the considerable progress in phase characterization, the early precipitation sequence is still far from being understood and much work remains to be done before the non-equilibrium phase diagram for the Al–Mg–Si system can be completed.

A more detailed understanding of nucleation and precipitation will have to involve computer simulations at the atomic scale. The initial stages of heterogeneous nucleation occur at the nano-scale level and therefore an accurate description of atom dynamics is needed to describe the precise growth kinetics. Intrinsic to such processes is the presence and diffusion of vacancies and vacancy–impurity complexes. For example, the extent to which vacancy-rich clusters play a role in the transformation to the GP 2 phase requires detailed experimental and theoretical study.

In the present work we investigate the structural properties of the equivalent bulk structure of the β''-crystallography identified by [5,6]. Since no accurate empirical model exists which describes the Mg–Si atomic interactions, we employ an *ab initio* density functional theory (DFT) technique to determine the interatomic forces, specifically the full-potential linear augmented-plane-wave (FLAPW) method. Moreover, by calculating the spatial distributions of the electronic charge density and transfer, we investigate some aspects of the nature of the bonding within the bulk β''-phase. We then propose a candidate face-centred-cubic (FCC) bulk Mg_5Si_6 structure from which the β''-phase can be obtained via a change in position of just one Mg atom and subsequent atomic structural relaxation.

2. The refinement of the β''-structure and its electron microscopy

Determination of the crystal structure of the β''-phase started with finding an atomic model from exit waves that were reconstructed from high-resolution electron microscopy (HREM) images of the small needle-shaped precipitates. The advantage of using exit waves is that information about atomic positions and Z-contrast is more accurate. Figure 1(a) shows an exit wave image of the β''-phase in which, for illustration purposes, the contrast has been further improved by a twofold averaging. The local thickness is 30–50 Å and white spots (atoms) are projections of atomic columns each with about ten atoms. The indicated 2.025 Å distance, half an Al unit-cell length, is between atoms at different heights. The actual distance between atoms is therefore 2.86 Å. In this figure we look down a β''-needle that is embedded in Al. The needle axis is parallel to the crystallographic b-axis of β'' and normal to the paper plane. This plane is spanned by the basis vectors a and c having a separation angle $\beta \approx 105.3^\circ$. The repeat distance along the needle (β-axis) is the same as for Al; thus $b = 4.05$ Å. The a-axis as indicated in figure 1(a) covers two periods. This is because the cell is C-centred and the atomic motif is accordingly shifted by $a/2 + b/2$. To summarize, the conventional β''-cell is a C-centred monoclinic structure with $a = 15.16$ Å, $b = 4.05$ Å, $c = 6.84$ Å, and $b \approx 105.3^\circ$. It is fully coherent with Al along the b-axis.

The sketch of the atomic structure model of β'' (figure 1(b)) has the same scale as the image. Large/small circles represent Mg/Si atoms. The two identical layers of the unit cell are differently shaded (see also figures 4 and 5 for a better view of the four-atom structure). For comparison, in figure 1(c) a similar image from a GP 1 zone is given. Here the Mg and Si atoms are distributed over the Al matrix positions. In Marioara *et al* [7], the most visible feature is the four atoms of high contrast (bright) arranged in a square. They would be a square of Al or Mg atoms centred above an Mg atom, as shown in figure 1(d). The central Mg atom

Table 1. Refined coordinates of β''-Mg_5Si_6 as determined from structural refinements and HREM [5, 6]. Atomic positions are given with respect to the monoclinic a- and c-axes. In parentheses we give the converged coordinates following *ab initio* relaxation of the atomic positions.

Atom	a	c
Mg1	0.0	0.0
Mg2	0.3459 (0.3456)	0.089 (0.0695)
Mg3	0.430 (0.4223)	0.652 (0.6375)
Si1	0.0565 (0.0550)	0.649 (0.6630)
Si2	0.1885 (0.1946)	0.224 (0.2519)
Si3	0.2171 (0.2063)	0.617 (0.6280)

is the main difference between the two structures. When this is 'moved' up or down one layer (2.025 Å) in the β''-structure, the atoms become arranged on a distorted FCC array. The GP 1 zone is in this way best described as an ordered superstructure on the Al FCC backbone.

To verify the atomic model of the β''-structure arrived at by analysing exit waves, refinements were done using data from electron diffraction (ED) patterns of the precipitates. Patterns with diffraction intensities had been obtained along the b-axis of β'' and along a direction normal to b. A total of 377 reflections were used in the refinement. Due to the strong interaction of the incident electrons with the crystal potential (even though the thickness involved was less than 200 Å) the software had to make corrections for dynamical scattering. The atomic coordinates of the model were refined using a multi-slice method combined with a least-squares algorithm [11, 12]. In addition, the actual thickness of the crystal for an ED pattern and the crystal orientation were refined. The relaxation of coordinates during the refinement showed no essential differences between the space groups $C2/m$, $C2$, Cm, and P. Thus the highest-symmetry space group $C2/m$, was chosen. Table 1 lists the coordinates of the structure. A final refinement of the temperature factors gave a slight improvement in the commonly used R-factor [11, 12]. The temperature factors all fall into a natural range. The program however only considers isotropic temperature factors. In the β''-phase there are several, possibly covalent Si–Si bonds and non-isotropic temperature factors might be expected, which could cause minor deviations from the atomic coordinates arrived at. In the light of this, a full theoretical relaxation of the structure using *ab initio* techniques is therefore very interesting.

3. The FLAPW method

In the present work the *ab initio* atomic structural relaxation calculations are based on the local density approximation within the DFT formalism [13, 14] in which the Kohn–Sham equations [15] are solved self-consistently. Here the FLAPW method is employed, which is similar to the LMTO approach of dividing the conventional cell into muffin-tin spheres (centred on the atomic sites) and an interstitial region. The underlying advantage of the FLAPW method (compared with traditional LMTO) is that within the muffin-tin spheres, no shape approximation is made to the potential or charge density, and in the interstitial region, no volume average is taken. This approach is thus ideally suited to studying charge-density profiles where charge pile-up between (Si) atoms can be used as an indicator that covalency is at play. For the present calculations the muffin-tin radius R_{mt} for both Si and Mg was chosen to be 2.0 au, and for the angular momentum expansion, $l_{max} = 10$ is used. A value $R_{mt}K_{max} = 6.0$ was used where K_{max} is the plane-wave cut-off. This is somewhat low for accurate total-energy calculations; however, for atomic relaxation studies and the production

of charge-density maps this was found to be sufficient. For the Brillouin zone integration a 26-special-point mesh was used. The software used for the present work is the Wien97 code developed by Blaha *et al* [16].

We should emphasize that all calculations were performed on the equivalent Mg_5Si_6 bulk structure within the conventional monoclinic base-centred cell. Thus, the roles and effects of the bulk Al matrix and Mg_5Si_6/Al matrix interface are not considered in the present work.

4. Charge-density profiles

In what follows we use a Cartesian coordinate system in which the origin is centred at the high-symmetry Mg1 atom. The x-axis is then chosen to be parallel to a, the z-axis to b, and the y-axis to $(c + a\cos\beta)$ (see table 1). Thus the z-axis is parallel to one of the equivalent Al FCC matrix $\langle 100\rangle$ axes, which we shall refer to as [001]. In all charge-density figures, the actual sizes of the Mg and Si atoms are not apparent since only the valence charge density is plotted.

Figure 2(a) shows a contour plot of the valence charge density in the plane normal to the z-axis, at $z = 1/2$ (i.e. $(b/2)$). Thus the view is down the [001] direction in the Cartesian coordinate system introduced (cf figure 1(a)). The central structure here is a chain of six Si atoms extending in the direction of the x-axis. Charge pile-up along the five respective bond axes indicates that the Si–Si covalent bond may be operative along the chain length. This would not be surprising since locally there is some degree of tetrahedral coordination, as well as the Si bond lengths (from left to right) being 2.61, 2.50, 2.29, 2.50, and 2.61 Å, where the bond length for bulk diamond cubic (DC) Si is 2.35 Å. The maximum charge density occurs at the central bond between Si1 atoms 3 and 4, and correlates with the corresponding bond length being the shortest of the sextet (3.5% less than for bulk silicon). Figure 2(c) displays the charge density in the $z = 0$ plane. Here the central feature is now a doublet triangle of Mg. This feature is of course also evident in figure 2(a) although translated by $a/2$ across the cell boundary. We see that the charge density in the region is relatively homogeneous, indicating an essentially metallic environment for the Mg with a bond length differing little from that of bulk HCP Mg.

Figure 2(b) shows the charge density in the $z = 1/4$ plane, halfway (in the z-direction) between those of figures 2(a) and (c). Two charge-density features become evident. The position and density magnitudes of those marked by an A indicate a similar charge pile-up between Si atoms 1, 2, 5, 6 of figure 2(a) and the respective Si atoms 6, 5, 2, 1 of the equivalent Si chain in figure 2(c), suggesting that covalency is also operative along the [100] direction. The concentration of charge at the regions indicated by B arises from the electron charge-density tails around the Si1 atom which sit directly above, in the $z = 0$ plane.

To confirm that the observed charge pile-up in the Si–Si bond regions originates due to a transfer of charge within the unit cell from the starting isolated atomic valence charge-density distribution (and not simply due to an overlap of atomic valence charge densities), we show in figure 3 the charge-density difference between the (DFT) converged charge density and the isolated atomic charge densities used as the initial guess for the DFT procedure. The orientations of the figures are the same as those in figure 2. Here we clearly see that there has indeed been a transfer of charge to all the Si–Si bond regions in which the bond distance is similar to that of bulk Si. What also becomes evident with such a figure is that there exists a transfer of charge to the region between the Si1 and Mg1 atoms, and to a lesser extent between Si3 and Mg1 (indicated by black arrows in figure 3(a)). Finally, if one considers a line joining two Si atoms (or a Si atom and a Mg1 atom), the regions along this line but on the opposite side to the Si atoms experience a decrease in charge. This is a typical feature of sp hybridization

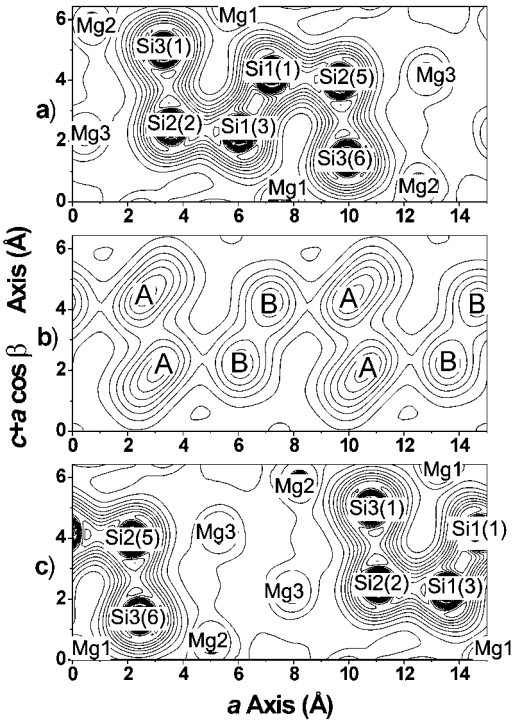

Figure 2. A contour plot of the valence charge density in the a–c plane at (a) $z = 0$, (b) $z = 1/4$ (i.e. $b/4$), and (c) $z = 1/2$ (i.e. $b/2$). The orthogonal Cartesian coordinate system described in section 4 is used.

in which the bonding state has a lobe which is significantly extended along one direction, at the expense of the opposite-side lobe.

These observations seem to suggest that there does exist a network of covalently bonded atoms throughout the Mg_5Si_6 structure. For example, Si1(4) is in an environment indicative of a sp^2 bonding geometry in the 100 plane of figure 4(a), having intra-plane bonding with Si2(5) (2.29 Å) and Si1(3) (2.50 Å), forming a bond angle of 116.0° with the remaining (dangling) bond which is terminated by the Mg1 atom (2.75 Å). The corresponding bond angles are Si1(4)–Si2(5)–Mg1 = 127.6° and Si1(4)–Si1(3)–Mg1 = 116.4°. For comparison, the bulk Si tetrahedral bond angle is 109.5°. On the other hand, Si2(2) is in an environment more indicative of sp^3 bonding geometry, bonding with Si1(3) (2.50 Å) and Si3(1) (2.61 Å) in the same 100 plane with a bond angle of 100.7°, and the two equivalent Si3(6) atoms (2.55 Å) in the lower $z = 0$ plane and the upper $z = 1$ plane. Here the bond angles are Si2(2)–Si3(1)–Si3(6-upper/lower) = 111.2°, Si2(2)–Si3(6-upper)–Si3(6-lower) = 105.2° and Si2(2)–Si1(3)–Si3(6-upper/lower) = 114.3°. The remaining unique local Si environment is that of Si3(1) which bonds covalently with that of Si2(2) (2.61 Å) in the same (100) plane, and with the equivalent Si2(5) atoms (2.55 Å) in the lower and upper z-planes forming bond angles of Si3(1)–Si2(2)–Si2(5-upper/lower) = 67.0° and Si3(1)–Si2(5-upper)–Si2(5-lower) = 105.5°. Thus, for Si3(1), the local bonding geometry with respect to the nearest-neighbour silicon atoms is not so tetrahedral. As already mentioned, there is however charge transfer to the region between Si3 and Mg1 (although less than that between Si1 and Mg1) indicating some directionality to the bonding. The Mg1 atom is at a distance of 2.86 Å from Si3(1), whereas

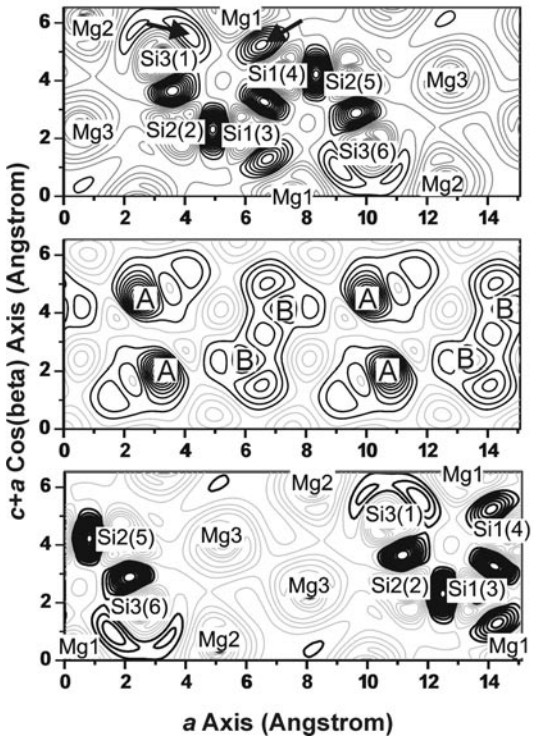

Figure 3. A contour plot of the valence charge-transfer density in the a–c plane at (a) $z = 0$, (b) $z = 1/4$ (i.e. $b/4$), and (c) $z = 1/2$ (i.e. $b/2$). The orthogonal Cartesian coordinate system described in section 4 is used. Here the dark contours represent positive charge transfer and the light-grey ones represent a negative transfer of charge.

the (nearest) Mg2 atom is a distance of only 2.77 Å from Si3(1) with little charge transfer to their mutual bonding region.

Thus we conclude that bulk β'' contains a two-dimensional-like filamentary structure of covalently bonded silicon in the a–b planes (normal to the y-axis), with some covalency, in the c-direction, between each pair of such layers via the Mg1 atom. Figure 4 shows the model structure (a) from the viewpoint of the [001] direction and (b) slightly off the [010] direction, where the Si–Si nearest-neighbour covalent bonds have been indicated along with those involving the Mg1 atoms. The dark dashed lines between the high-symmetry Mg1 atom and the surrounding Si atoms represent the observation of some directional bonding between these atoms, and thus between the differing Si covalent filamentary structures.

5. Atomic relaxation

For the refined coordinates given in table 1, the converged FLAPW calculation gives non-zero Hellmann–Feynman forces for all but the high-symmetry Mg1 atom which has identically zero forces due to it being at a site with inversion symmetry. The average magnitudes of the Hellmann–Feynman forces for the refined atomic coordinates were approximately 30 mRyd $Å^{-1}$ in the a–c plane. They are identically zero in the b-direction (z-axis direction) due to the mirror plane symmetry. Although small, the non-zero forces are not negligible.

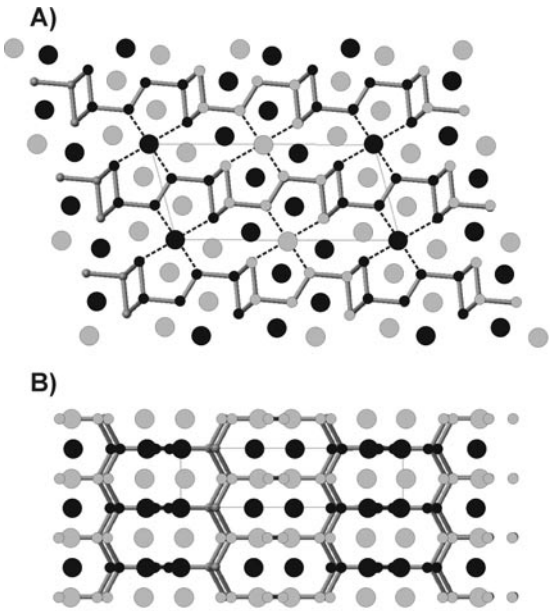

Figure 4. A model of the β''-structure in which covalent bonds between the silicons are displayed as light-grey cylinders and those between the magnesium and silicon as dashed lines. The magnesium and silicon atoms are displayed using the same symbols as in figures 1(*b*) and (*d*). (*a*) displays the structure from the [001] Cartesian direction (along the *b*-axis of β'') revealing layered networks of covalently bonded Si. (*b*) displays the same structure from slightly off the [010] Cartesian direction, showing that each layer appears as a stretched honeycomb structure filled with metallic Mg.

To investigate the effect of these forces on the refined atomic positions, we relax the structure within the $C2/m$ symmetry, by performing a Newton–Cotes energy-minimization procedure with respect to the five non-equivalent atoms. Table 1 lists the converged relaxed positions of the non-equivalent atoms in parentheses. A cursory inspection of the corresponding charge-density maps for the relaxed structure reveals that for the silicon substructure the nearest-neighbour (Si–Si) distances are now closer to those of bulk silicon, with the Si sextet (see figure 2(*a*)) having the respective distances 2.53, 2.36, 2.41, 2.36, and 2.53 Å. In addition, all Si–Si bond angles are shifted towards the tetrahedral bond angle. Together, these features result in a more even distribution of charge over the covalently bonded Si structure.

The $C2/m$ space group has a twofold symmetry within the *a–c* plane due to Mg1 having inversion symmetry, whereas the mirror plane arises from the atoms lying exactly in the $z = 0$ and $z = 1/2$ *b*-planes. By removing the requirement of inversion symmetry, we break the twofold rotation symmetry, consequently obtaining the C/m space group. Under these conditions eleven rather than five atoms are free to move in the *a–c* plane. On allowing these atoms to move off the *a–c* plane, the mirror plane symmetry is broken, resulting in the $C2$ space group if inversion is maintained, or the C space group if the twofold rotation symmetry is abandoned. In what follows we consider structural relaxation within the $C2$ and C space groups.

We thus repeat the structural relaxation, now with the starting configuration of eleven atoms being randomly perturbed from their refined positions. For the $C2$ calculation the perturbations occurred within the *a–c* plane, and only broke the twofold symmetry. For the C calculation, the random perturbations were fully three dimensional, and also broke the mirror plane symmetry. The mean square distances between the perturbed starting configuration and

Table 2. Relaxed coordinates of β''-Mg_5Si_6 determined from *ab initio* relaxations within the full $C2/m$ symmetry, as well as the $C2$ symmetry (no inversion symmetry) and C symmetry (no inversion and mirror plane symmetry). The coordinates are given in ångströms with respect to a Cartesian coordinate system (see section 4) with the origin taken as the location of the Mg1 atom in each symmetry.

	Refined	Relaxed ($C2/m$)	Relaxed ($C2$)	Relaxed (C)
Mg2	5.083	5.113	5.083	5.092
	0.587	0.459	0.464	0.472
	0.0	0.0	0.0	0.011
Mg2′			5.064	−5.073
			0.435	−0.443
			0.0	0.014
Mg3	5.340	5.251	5.238	5.244
	4.302	4.206	4.181	4.188
	0.0	0.0	0.0	−0.010
Mg3′			−5.216	−5.214
			4.174	−0.443
			−0.0	−0.014
Si1	−0.315	4.282	0.0	−0.364
	4.374	0.0	−0.366	4.389
	0.0	−0.362	4.390	−0.030
Si1′			0.395	−4.371
			0.0	0.396
			−4.369	0.030
Si2	2.453	1.478	0.0	2.495
	1.662	0.0	2.507	1.695
	0.0	2.511	1.688	−0.011
Si2′			−2.485	−1.672
			0.0	−2.485
			−1.667	0.001
Si3	2.178	4.071	0.0	1.993
	4.144	0.0	2.009	4.204
	0.0	2.014	4.197	−0.001
Si3′			−1.981	−4.182
			0.0	−1.981
			−4.176	−0.009

$C2/m$ refined coordinates were typically greater than those encountered due to thermal motion. Table 2 lists the converged atomic positions for the different symmetries, along with the refined coordinates. In this table, coordinates are in the Cartesian coordinate system introduced in section 4, and given in ångströms with the origin taken as the location of the Mg1 atom in each symmetry. We see that with a reduction of symmetry there exists only a small change in atomic positions. Indeed for both $C2$ and C, inversion symmetry is largely maintained, the centres of the positions being respectively 1.36×10^{-2} and 1.57×10^{-2} Å. For the C case, the atomic positions relaxed towards the mirror plane. Thus the primary relaxation has occurred in going from the refined to the relaxed coordinates, with only minor relaxation by lowering of the unit-cell symmetry.

The β''-structure can also be visualized in part, from the perspective of a base-centred monoclinic array of BCC Mg, capped with silicon above the face centres of the a–c plane (figure 5). This more symmetric structure was used as an initial guess (input) for the structural

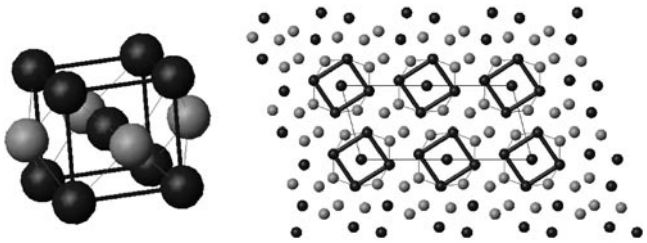

Figure 5. The β''-structure can be seen as a base-centred monoclinic array of slightly distorted body-centred Mg cells having Si capped above the face centres. The light-grey balls represent silicon and the dark-grey ones represent magnesium. This exact structure was used as an initial guess in the ED structure refinement procedure as detailed in section 2.

Table 3. The proposed FCC array of Mg_5Si_6. Atomic positions are given with respect to the a–c coordinate system in fractions of the corresponding axes.

Atom	a	b	c
Mg1	0.0	0.5	0.0
Mg2	0.318 18	0.0	0.090 909
Mg3	0.409 09	0.0	0.545 454
Si1	0.045 45	0.0	0.727 273
Si2	0.136 36	0.0	0.181 818
Si3	0.227 27	0.0	0.636 364

refinement process used in [5,6], the coordinate positions of the Mg and Si refining back to those published. The final relaxed coordinates (in table 3) for the lower symmetries more closely approach this structure, indicating relaxation towards a more symmetric configuration, with the Mg atoms forming a more symmetric body-centred cube. One does not expect this to be ideal, due to the additional silicon (needed to complete the β''-structure) breaking the symmetry.

6. The pre-β''-to-β'' precipitation transformation

The precise nucleation or transformation leading to the β''-phase is still largely unknown. It is assumed that the pre-β''-phase, the so-called GP 1 zone, undergoes some kind of structural transformation. This phase occurs as even smaller needles of Mg and Si, the cross-section spanning a few unit cells (see figure 1(c)), and with a length of a few tens of ångströms, which through the appropriate diffusion kinetics will transform/grow to the macroscopically relevant β''-needles. Due to the smallness and the perfect coherency with the Al matrix, such structures are generally beyond detection via HREM and the corresponding structural refinement process used to determine the β''-crystallography. Their presence is however evident [7], where an atomic model can be inferred from exit wave images. In the present work we explore some possibilities for the origin of the atomic arrangement within β''.

What can be assumed with confidence is that after quenching the Al–Mg–Si solid solution, vacancy-assisted diffusion induces the nucleation and growth of predominantly Mg–Si phases with the bulk Al FCC matrix remaining initially intact. It is known that in the Al–Si alloy system, the Si are quickly attracted to each other, again within the Al FCC matrix. Such (small) FCC clusters of Si become unstable with increasing size and transform into the DC structure (an FCC array of Si being a metal with a less negative cohesive energy than that for the DC structure). Generally it is known that if additional atoms are attracted to the Si clusters, the DC structure is replaced by typical intermetallic compound structures such as Mg_2Si.

Thus two distinct approaches may be applicable to the present problem. Either β'' transforms/grows from small clusters of Si in the DC phase, or it arises directly from a bulk (Al) FCC arrangement of Mg and/or Si. At first glance, the former may seem more likely since the critical diameter at which there is a Si FCC/Si DC transformation in Al–Si is rather small (<10 Å) due to large internal stresses. In Al–Mg–Si, however, Mg and vacancies are quickly attracted to such sites, reducing the stress and allowing for a larger critical size [17]. Thus, beginning from a FCC arrangement of atoms is perhaps the wiser choice and, in addition, such an approach is supported by a recent experiment [7] that indicates the early presence of the Mg1 supercell within the Al FCC matrix.

Clearly, the roles played by vacancies and Al must be crucial to the existence of β'', especially at the interface region which at the nanometre scale becomes less well defined. In the present work we consider the β''-phase to arise directly from a FCC array of Mg and Si. This should be regarded as an ideal 'foundational' pre-β''-structure, for it ignores the presence of Al and thus implicitly the role of the Al FCC–pre-β'' interface. Thus the candidate structure for the present work consists of Mg and Si atoms distributed in a FCC (backbone) matrix with a lattice constant chosen to be equal to that of bulk Al, 4.05 Å. The chosen distribution of Mg and Si forms a conventional cell which is a base-centred monoclinic one with cell parameters determined from the Cartesian basis vectors of bulk Al (a_{Al}, b_{Al}, c_{Al}):

$$a = 2a_{\mathrm{Al}} + 3c_{\mathrm{Al}} \qquad b = b_{\mathrm{Al}} \qquad c = -\tfrac{3}{2}a_{\mathrm{Al}} + \tfrac{1}{2}c_{\mathrm{Al}}. \tag{1}$$

This gives respective side-lengths of 14.6, 4.05, and 6.4 Å with a monoclinic angle β of 105.3°. These are comparable to the β''-unit-cell parameters given in section 2. Table 3 details the atomic positions within the $C2/m$ symmetry and we see that there are no great differences in the a–c plane atomic positions, apart from the Mg1 atom now being shifted by $b/2$ to accommodate the correct FCC lattice sites. This structure can be most easily visualized by inspection of the left-hand side of figure 5: to obtain the proposed FCC structure from the β''-structure, the body-centred Mg atom is shifted upwards to the top face-centred location, while the capped Si atoms are shifted into the nearby face centres. From this perspective, the proposed structure is not that different to the GP 1 cluster in [7] without Al.

We repeated the *ab initio* atomic relaxation procedure on this lattice in the way outlined in section 5. This was also repeated using the (lower) symmetries detailed in section 6, where all initial starting coordinates were again perturbed. For brevity, we however only detail the case for the full $C2/m$ symmetry, which describes the dominant atomic relaxations. Figure 6(a) displays the resulting relaxed charge-density distribution in the a–c plane and reveals that the still FCC arrangement of Si is indeed metallic due to the absence of charge pile-up along the Si–Si bond length (for comparison to bulk FCC Si *ab initio* calculations, see [18]). To aid in visualization, the same atomic labelling as was used in figures 2 and 3 has been employed. Whilst maintaining all other unrelaxed atomic positions, we now shift the Mg1 atom down by $b/2$ and repeat the *ab initio* relaxation procedure. The final relaxed atomic positions of this structure are listed in parentheses in table 3, and the corresponding charge-density map is shown in figure 6(b). Inspection clearly reveals that the relaxed structure is not that different from the original β''-configuration (see table 1 and also the charge-density plot in figure 2). Differences are of course expected due to the slightly different conventional cell parameters; however, we may conclude that the β''-phase is reproduced.

7. Concluding remarks

The elucidation of the covalent substructure within the β''-phase suggests a significant mechanical anisotropy, with a predominantly covalent structure existing along the b-axis. It is

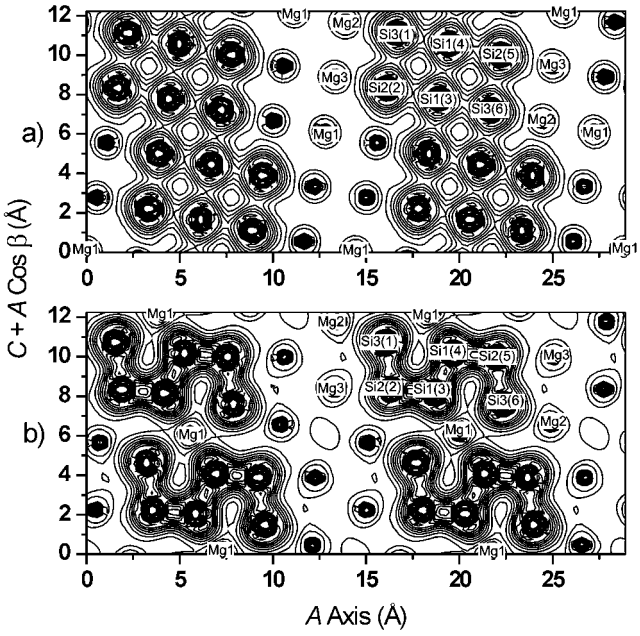

Figure 6. (*a*) The calculated charge-density map of the candidate array of Si and Mg based on a FCC backbone lattice. Here the position of Mg1 is significantly different from that of the β''-position, to accommodate the appropriate FCC site (see table 4). The charge density within the silicon region indicates an essentially metallic environment. (*b*) The calculated charge density of the relaxed structure with Mg1 shifted down by $b/2$; we see that the resulting structure is not that different from the β''-structure. In both figures atoms from four C-centred monoclinic conventional cells are displayed, and for one unit cell the atomic labelling is that used in figures 2 and 3.

not difficult to imagine the theoretical shear strength being much greater along this direction than that along the a-axis, where there is significantly less covalency at play. We note that the b-axis coincides with the direction of the experimentally seen β''-needles in the Al matrix that act as dislocation pinning sites and contribute to the increase in hardness of the alloy system. Atomic relaxation of the experimentally obtained atomic structure demonstrated a more symmetric structure that survives under atomic perturbations, which broke both the inversion and mirror plane symmetry of the $C2/m$ space group. The final converged structure was not that different from the original guess used in the experimental structural refinement work. In the original work of Zandbergen, Andersen and co-workers [5, 6] a spherical Debye–Waller approximation was used to account for the atomic vibrations. The present work, however, suggests that such an assumption may not be justified due to the strongly covalent nature of the Si and a more accurate structural refinement procedure may need to take into account more anisotropic Debye–Waller contributions, perhaps through an ellipsoidal approximation.

The present work does not consider relaxation of the unit cell. Indeed, ideally, the atomic force and unit-cell stress should be minimized in parallel. Such a calculation using the DFT technique can be performed in a similar way to that outlined by Mehl *et al* [19]. However, very accurate total-energy calculations are needed as a function of unit-cell distortions, especially for the volume-conserving monoclinic distortions. The applicability of such a calculation is questionable since the experimentally obtained unit-cell parameters used here are extremely accurate, and determined from Mg_5Si_6 needles existing in the Al matrix, where the Mg_5Si_6–Al

interface may play an important stabilizing role. Furthermore, the local density approximation used in the present DFT calculation is known to underestimate the converged unit-cell lattice constants.

Finally we investigated an ordered Mg_5Si_6 $C2/m$ structure on a FCC array. This can be viewed as an infinite supercell structure of only Mg and Si atoms and an idealized model for the GP 1 phase. Such an array is similar to the β''-phase apart from different interatomic distances, and except that one Mg position (Mg1) is displaced by $b/2$ to a neighbouring y-plane (b-plane). Atomic relaxation shows that this FCC matrix is retained within the $C2/m$, $C2$, and C symmetries—all atoms remaining in an essentially metallic environment. By then shifting the Mg1 atom by $b/2$ to the corresponding β''-positions whilst keeping the remaining atoms on a FCC grid, and repeating the atomic relaxation calculation again for the $C2/m$, $C2$, and C symmetries, we find that the β''-phase is reproduced.

The calculated energy difference (using the energy cut-off and k-space mesh described in section 3) between the two relaxed structures is 0.044 eV/atom—with the β''-structure being the more stable. Since, the position of Mg1, for both structures, maintains the general inversion symmetry (under $C2/m$ and C/m), there exists a potential barrier between the FCC matrix of Mg and Si, and the β''-structure. Thus the bulk transformation would be a thermal process. Further work would be required to calculate the precise barrier energy between the two phases; however, it is likely that a more local pathway exists, thus defining an atomic migration energy for the transformation. A variety of possibilities may occur to facilitate such a process. For example the presence of vacancies at or around the FCC Mg1 sites will lead to its diffusion. Alternatively, the role of the Al FCC–β'' interface may play a crucial role in the transformation to the β''-structure.

In conclusion, the precise transformation sequence to β'' may manifest itself though the mechanism by which the Mg1 atom shifts to the interstitial region with respect to the original FCC backbone lattice. The role played by Al is most probably relegated to the FCC/β'' interface region, since Al is believed to be quickly ejected from clusters of Si [18], and is not present in the late-stage intermetallic precipitate phases of Al–Mg–Si. In the work of Marioara *et al* [7] such FCC arrays of Mg and Si are also identified from HREM images of small Mg–Si clusters in which Al atoms are nevertheless proposed. For small Mg–Si nuclei, the interface and bulk region become less defined, and Al may well play a more general and important role in the early growth kinetics. Thus we conclude that the GP 1–β'' transformation may be a simple, low-energy phase transformation without compositional changes.

Acknowledgments

PMD acknowledges the financial support of the Norwegian Research Council (grant no 116559/431). SJA and CDM acknowledge Norsk Hydro, Metallurgical Research and Development Centre, Sunndalsøra, Norway, for financial support and cooperation. CDM acknowledges financial support from Delft University of Technology, The Netherlands. AF acknowledges the financial support of the Norwegian Research Council grant no 143877/213 and Norsk Hydro.

References

[1] Dutta I and Allen S M 1991 *J. Mater. Sci. Lett.* **10** 323
[2] Lutts A 1961 *Acta Metall.* **9** 577
[3] Panseri C and Federighi T 1966 *J. Inst. Met.* **94** 99
[4] Shchegoleva T V 1968 *Phys. Met. Metallogr.* **25** 56

[5] Zandbergen H W, Andersen S J and Jansen J 1997 *Science* **277** 1221
[6] Andersen S J, Zandbergen H W, Jansen J, Truholt C, Tundal U and Reiso O 1998 *Acta Mater.* **46** 3283
[7] Marioara C D, Andersen S J, Jansen J and Zandbergen H W 2001 *Acta Mater.* **49** 321
[8] Edwards G A, Stiller K, Dunlop G L and Couper M J 1998 *Acta Mater.* **46** 3893
[9] Murayama M, Hono K, Saga M and Kikuchi M 1998 *Mater. Sci. Eng.* **A250** 127
[10] Marioara C D, Jansen J, Zandbergen H W and Andersen S J 2001 submitted
[11] Jansen J, Tang D, Zandbergen H W and Schenk H 1998 *Acta Crystallogr.* **A54** 91
[12] Zandbergen H W, Bokel R, Connolly E and Jansen J 1999 *Micron* **30** 395
[13] Hohenberg P and Kohn W 1964 *Phys. Rev.* B **136** 864
[14] Perdew J P and Wang Y 1992 *Phys. Rev.* B **45** 13 244
[15] Kohn W and Sham L J 1965 *Phys. Rev.* A **140** 1133
[16] Blaha P, Schwarz K, Dufek P and Augustyn R 1999 *WIEN97, a Full Potential Linearized Augmented Plane Wave Package for Calculating Crystal Properties* Karlheinz Schwarz, Technical University of Vienna
This is an updated version of the code originally published by
Blaha P, Schwarz H, Sorantin P and Trickey S B 1990 *Comput. Phys. Commun.* **59** 399
[17] Hornbogen E, Mukhopadhyay A K and Starke E A 1993 *J. Mater. Sci.* **28** 3670
[18] Lui A Y, Chang K J and Cohen M L 1988 *Phys. Rev.* B **37** 6344
[19] Mehl M J, Klein B M and Papaconstantopoulos D A 1994 *Principles (Intermetallic Compounds vol 1)* ed J H Westbrook and R L Fleischer (New York: Wiley) p 195